The 8th European Congress on Computational Methods in Applied Sciences and Engineering
ECCOMAS Congress 2022
5-9 June 2022, Oslo, Norway

INVERSE DYNAMICS OF GEOMETRICALLY EXACT BEAMS

TIMO STRÖHLE AND PETER BETSCH

Institute of Mechanics
Karlsruhe Institute of Technology, Karlsruhe, Germany
timo.stroehle@kit.edu, peter.betsch@kit.edu

Key words: Inverse dynamics, Galerkin space-time integration, Method of characteristics, Geometrically exact beam formulation, Wave propagation

Abstract. This paper is concerned with the inverse dynamics of flexible mechanical systems whose motion is governed by quasi-linear hyperbolic partial differential equations. Problems that appear by applying classical solution strategies to the problem at hand, e.g. integrating the problem at hand sequentially in space and time will be adressed in this work. Motivated by the hyperbolic structure of the underlying initial boundary value problem, two methods that are based on a simultaneous space-time integration will be presented. Special emphasize will be given to the phenomena of wave propagation within geometrically exact beams and its relevance regarding the inverse dynamics problem.

1 PROBLEM

The focus of this work lies on the inverse dynamics of spatially continuous (infinite dimensional) mechanical systems where the motion is governed by partial differential equations of the form

$$\boldsymbol{A}\partial_t^2\boldsymbol{x} - \partial_s(\boldsymbol{B}\partial_s\boldsymbol{x}) = \boldsymbol{C}. \tag{1}$$

Since we are interested in quasi-linear equations, we explicitly allow the functions $\boldsymbol{A}$, $\boldsymbol{B}$ and $\boldsymbol{C}$ to depend on the solution $\boldsymbol{x} : \Omega \mapsto \mathbb{R}^d$ itself, as well as on their first partial derivatives such that

$$\boldsymbol{A}, \boldsymbol{B} : \bar{\Omega} \mapsto \mathbb{R}^{d,d} \qquad \text{and} \qquad \boldsymbol{C} : \bar{\Omega} \mapsto \mathbb{R}^d \qquad \text{where} \qquad \bar{\Omega} = \Omega \cup \{(\boldsymbol{x}, \partial_s\boldsymbol{x}, \partial_t\boldsymbol{x}) : \Omega \mapsto \mathbb{R}^d\}.$$

Here, $\Omega = S \times T$ denotes the space-time domain, where $S \subset \mathbb{R}$ represents the spatial and $T \subset \mathbb{R}^+$ the temporal domain. Furthermore, the equation at hand is subjected to given initial conditions on $\partial\Omega_0 = S \times \{0\}$

$$\boldsymbol{x}(\partial\Omega_0) = \boldsymbol{x}_0, \qquad \partial_t\boldsymbol{x}(\partial\Omega_0) = \boldsymbol{v}_0 \tag{2}$$

and to Neumann boundary conditions on $\partial\Omega_f = \{0\} \times T$

$$\boldsymbol{B}\partial_s\boldsymbol{x}(\partial\Omega_f) = \boldsymbol{f}(t) \tag{3}$$

and on $\partial\Omega_h = \{1\} \times T$

$$\boldsymbol{B}\partial_s\boldsymbol{x}(\partial\Omega_h) = \boldsymbol{h}(\partial_t^2\boldsymbol{x}(\partial\Omega_h), \partial_t\boldsymbol{x}(\partial\Omega_h), \boldsymbol{x}(\partial\Omega_h), t). \tag{4}$$

Note that $\boldsymbol{h}$ may denote an ordinary differential equation. For the inverse dynamics, the system is additionaly subjected to the following time-varying Dirichlet boundary condition on $\partial\Omega_h$

$$\boldsymbol{x}(\partial\Omega_h) = \boldsymbol{\gamma}(t). \tag{5}$$

The task is to find the unknown functions $\boldsymbol{f} : \partial\Omega_f \mapsto \mathbb{R}^d$ and $\boldsymbol{x} : \Omega \mapsto \mathbb{R}^d$ such that (1)-(5) are satisfied.

Geometrically exact beam formulation. In the following, the *classical equations of motion of geometrically exact beams* are briefly derived. Furthermore it will be shown, that these equations indeed fit into the proposed framework introduced in the beginning of this Section. Essentially, these derivations are based on the work published in [1], [2], [3] and [4].

Kinematics. The motion of every material point $s \in S = [0, 1] \subset \mathbb{R}$ of the beam for every point in time $t \in T = [0, \infty) \subset \mathbb{R}$ is defined by the deformation map [1]

$$\boldsymbol{r} : \Omega \equiv S \times T \mapsto \mathbb{R}^3$$

together with the moving orthonormal basis

$$\boldsymbol{d}_i : \Omega \mapsto \mathbb{R}^3 \qquad \forall i \in \{1, 2, 3\}.$$

Furthermore, we define in the reference configuration

$$\boldsymbol{R}(s) \equiv \boldsymbol{r}(\partial\Omega_0) : \partial\Omega_0 \mapsto \mathbb{R}^3 \qquad \text{and} \qquad \boldsymbol{D}_i(s) \equiv \boldsymbol{d}_i(\partial\Omega_0) : \partial\Omega_0 \mapsto \mathbb{R}^3.$$

By introducing the proper-orthogonal tensor $\boldsymbol{\Lambda} \in SO(3)$, the rotation of the orthonormal basis is given by

$$\boldsymbol{d}_i = \boldsymbol{\Lambda}\boldsymbol{D}_i. \tag{6}$$

Note that the orthonormal basis $\boldsymbol{d}_i$ indicates the 'average orientation of the cross-section', whereby $\boldsymbol{d}_3$ is normal and $\boldsymbol{d}_1$ and $\boldsymbol{d}_2$ are tangential to the cross-section. It may be worth to emphasize at this point, that planarity of the cross-section is assumed. Abandoning this assumption would require a further spatial variable. A spatial differentiation of the moving frame yields

$$\partial_s\boldsymbol{d}_i = (\partial_s\boldsymbol{\Lambda})\boldsymbol{D}_i + \boldsymbol{\Lambda}\partial_s\boldsymbol{D}_i \quad = (\partial_s\boldsymbol{\Lambda})\boldsymbol{\Lambda}^T\boldsymbol{d}_i + \boldsymbol{\Lambda}(\partial_s\boldsymbol{\Lambda}_0)\boldsymbol{\Lambda}_0^T\boldsymbol{\Lambda}^T\boldsymbol{d}_i. \tag{7}$$

Here, use of the product rule and $\boldsymbol{D}_i = \boldsymbol{\Lambda}_0\boldsymbol{e}_i$ has been made. Introducing the skew-symmetric curvature matrix [2]

$$\boldsymbol{S}_{\boldsymbol{\kappa}}(\boldsymbol{\Theta}) = (\partial_s\boldsymbol{\Lambda}(\boldsymbol{\Theta}))\boldsymbol{\Lambda}^T(\boldsymbol{\Theta}) = \begin{bmatrix} 0 & -\kappa_3 & \kappa_2 \\ \kappa_3 & 0 & -\kappa_1 \\ -\kappa_2 & \kappa_1 & 0 \end{bmatrix} \tag{8}$$

equation (7) can be rewritten as

$$\partial_s\boldsymbol{d}_i = (\boldsymbol{S}_{\boldsymbol{\kappa}}(\boldsymbol{\Theta}) + \boldsymbol{\Lambda}\boldsymbol{S}_{\boldsymbol{\kappa}}(\boldsymbol{\Theta}_0)\boldsymbol{\Lambda}^T)\boldsymbol{d}_i = \bar{\boldsymbol{S}}_{\boldsymbol{\kappa}}(\boldsymbol{\Theta}, \boldsymbol{\Theta}_0)\boldsymbol{d}_i \tag{9}$$

[1] Note, that the deformation map $\boldsymbol{r}(\Omega)$ must not necessarily coincides with the line of centroids of the beam.

[2] Orthogonality of $\boldsymbol{\Lambda}$ implies $\boldsymbol{\Lambda}\boldsymbol{\Lambda}^T = \boldsymbol{I}$. Differentiation of this orthogonality condition with respect to s yields $\partial_s(\boldsymbol{\Lambda})\boldsymbol{\Lambda}^T + \boldsymbol{\Lambda}\partial_s(\boldsymbol{\Lambda}^T) = 0$ which indicates the skew-symmetry of $\partial_s(\boldsymbol{\Lambda})\boldsymbol{\Lambda}^T$

Note that assuming a straight reference configuration implies $\boldsymbol{S}_\kappa(\boldsymbol{\Theta}_0) = \boldsymbol{0}$. Introducing the axial vector $\boldsymbol{\kappa} = \kappa_i \boldsymbol{d}_i$, equation (9) can be defined alternatively as

$$\partial_s \boldsymbol{d}_i = \boldsymbol{\kappa} \times \boldsymbol{d}_i.$$

The same relations hold for the temporal change of the moving basis

$$\partial_t \boldsymbol{d}_i = \boldsymbol{S}_{\boldsymbol{\omega}}(\boldsymbol{\Theta}, \boldsymbol{\Theta}_0)\boldsymbol{d}_i = \boldsymbol{\omega} \times \boldsymbol{d}_i,$$

where $\boldsymbol{S}_{\boldsymbol{\omega}}$ represents the skew symmetric angular velocity matrix. Following [1], we define the strain variables $\gamma_i = \partial_s \boldsymbol{r} \cdot \boldsymbol{d}_i$ and κ_i, where γ_1 and γ_2 measure shear, γ_3 measures dilatation, κ_1 and κ_2 measure flexure and κ_3 measures torsion.

Example 1.1 *(Planar problem) Regarding planar motion, the rotation arround $\boldsymbol{d}_2(s,t) \equiv \boldsymbol{D}_2(s)$ for all $t \in T$ can be described by the following proper orthogonal matrix*

$$\boldsymbol{\Lambda} = \begin{bmatrix} \cos\Theta & 0 & -\sin\Theta \\ 0 & 1 & 0 \\ \sin\Theta & 0 & \cos\Theta \end{bmatrix}. \tag{10}$$

For the axial vector it applies $\boldsymbol{\omega} = \omega_2 \boldsymbol{d}_2 = \omega_2 \boldsymbol{e}_2$. This can be shown by simply using (10) *to compute the angular velocity matrix $\boldsymbol{S}_{\boldsymbol{\omega}}$*

$$\boldsymbol{S}_\omega = \partial_t(\boldsymbol{\Lambda})\Lambda^T = \partial_t\Theta \begin{bmatrix} -\sin\Theta & 0 & -\cos\Theta \\ 0 & 0 & 0 \\ \cos\Theta & 0 & -\sin\Theta \end{bmatrix} \begin{bmatrix} \cos\Theta & 0 & \sin\Theta \\ 0 & 1 & 0 \\ -\sin\Theta & 0 & \cos\Theta \end{bmatrix} = \partial_t\Theta \begin{bmatrix} 0 & 0 & -1 \\ 0 & 0 & 0 \\ 1 & 0 & 0 \end{bmatrix}.$$

The same can be shown for the curvature $\boldsymbol{\kappa} = \kappa_2 \boldsymbol{d}_2 = \kappa_2 \boldsymbol{e}_2$ by computing the curvature matrix in (8) *using* (10)

Equilibrium. After having adressed the kinematics in the last Section, the corresponding dynamics will be investigated in the following Section. The (material form of the) balance of linear momentum on an interval $S \supset I = [c, s]$ of the beam can be established as follows

$$\boldsymbol{n}(s,t) - \boldsymbol{n}(c,t) + \int_c^s \bar{\boldsymbol{n}}(\xi_3)\ \mathrm{d}\xi_3 = \partial_t \boldsymbol{P}(s,t). \tag{11}$$

Herein we defined the contact force $\boldsymbol{n} : \Omega \mapsto \mathbb{R}^3$, the external load $\bar{\boldsymbol{n}} : \Omega \mapsto \mathbb{R}^3$ and the linear momentum of the considered beam segment $\boldsymbol{P} : \Omega \mapsto \mathbb{R}^3$ which can be stated for the center of gravity $\boldsymbol{r}_S = \boldsymbol{r} + \xi_\alpha^S \boldsymbol{d}_\alpha$ as

$$\begin{aligned} \boldsymbol{P}(s,t) &= \int \partial_t \boldsymbol{r}_S\ \mathrm{d}m \\ &= \int_c^s (\rho A)(s)\partial_t \boldsymbol{r} + (\rho S_\alpha)(s)\partial_t \boldsymbol{d}_\alpha\ \mathrm{d}\xi_3 \qquad \forall \alpha \in \{1,2\} \\ &= \int_c^s \boldsymbol{p}(s,t)\ \mathrm{d}\xi_3. \end{aligned} \tag{12}$$

Here, we used the fact that the center of gravity of each cross-section is defined by the components $\xi_\alpha^S = A^{-1} \int \xi_\alpha \; \mathrm{d}A = A^{-1} S_\alpha$, where $S_\alpha \forall \alpha \in \{1, 2\}$ is the first moment of area with respect to ξ_α. Time derivative of the linear momentum yields

$$\partial_t \boldsymbol{p}(s,t) = (\rho A)(s) \partial_t^2 \boldsymbol{r} + \partial_t^2 \boldsymbol{q}. \tag{13}$$

Herein, use has been made of the definition of the linear momentum relative to $\boldsymbol{r}(s,t)$

$$\partial_t \boldsymbol{q}(s,t) \equiv (\rho S_\alpha)(s) \partial_t \boldsymbol{d}_\alpha \qquad \forall \alpha \in \{1, 2\}.$$

Obviously, the relative linear momentum vanishes by choosing $\boldsymbol{r}(s,t)$ accurate. Furthermore, for the same beam segment, the material form of the balance of angular momentum can be established in the form

$$\begin{aligned} &\boldsymbol{m}(s,t) - \boldsymbol{m}(c,t) + (\boldsymbol{r}(s,t) \times \boldsymbol{n}(s,t)) - (\boldsymbol{r}(c,t) \times \boldsymbol{n}(c,t)) \\ &\qquad + \int_c^s \boldsymbol{r}(\xi) \times \bar{\boldsymbol{n}}(\xi) \; \mathrm{d}\xi + \int_c^s \bar{\boldsymbol{m}}(\xi) \; \mathrm{d}\xi = \partial_t \boldsymbol{L}(s,t). \end{aligned} \tag{14}$$

Herein, we introduced the contact torque $\boldsymbol{m} : \Omega \mapsto \mathbb{R}^3$, the external applied torques $\bar{\boldsymbol{m}} : \Omega \mapsto \mathbb{R}^3$ and the angular momentum (with respect to a fixed point in space) of the considered beam segment $\boldsymbol{L} : \Omega \mapsto \mathbb{R}^\alpha$ which can be stated with $\boldsymbol{r}_P = \boldsymbol{r} + \xi_\alpha \boldsymbol{d}_\alpha$ as

$$\begin{aligned} \boldsymbol{L}(s,t) &= \int \boldsymbol{r}_P \times \partial_t(\boldsymbol{r}_P) \, \mathrm{d}m \\ &= \int_c^s \rho A(\boldsymbol{r} \times \partial_t \boldsymbol{r}) + \rho S_\alpha(\boldsymbol{r} \times \partial_t \boldsymbol{d}_\alpha + \boldsymbol{d}_\alpha \times \partial_t \boldsymbol{r}) + \rho I_\alpha(\boldsymbol{d}_\alpha \times \partial_t \boldsymbol{d}_\alpha) \; \mathrm{d}\xi_3 \\ &= \int_c^s \boldsymbol{l}(s,t) \; \mathrm{d}\xi_3. \end{aligned} \tag{15}$$

Herein, $\boldsymbol{l}(s,t)$ denotes the angular momentum density. Its time derivative is

$$\partial_t \boldsymbol{l}(s,t) = \rho A(\boldsymbol{r} \times \partial_t^2 \boldsymbol{r}) + \boldsymbol{r} \times \partial_t^2 \boldsymbol{q} + \boldsymbol{q} \times \partial_t^2 \boldsymbol{r} + \partial_t \boldsymbol{h} \quad , \tag{16}$$

where use has been made of the definition of the angular momentum relative to $\boldsymbol{r}(s,t)$,

$$\boldsymbol{h}(t) \equiv \rho I_{\alpha\beta}(\boldsymbol{d}_\alpha \times \partial_t \boldsymbol{d}_\beta)$$

and the standard properties of the vector product $\boldsymbol{a} \times \boldsymbol{b} = -\boldsymbol{b} \times \boldsymbol{a}$ and $\boldsymbol{a} \times \boldsymbol{a} = \boldsymbol{0}$ Furthermore, we have introduced the second moment of area $I_{\alpha\beta} = \int \xi_\alpha \xi_\beta \; \mathrm{d}A$. Differentiating (11) and (14) with respect to the spatial variable $s \in S$, the balance equations can be written as

$$\begin{aligned} \partial_s \boldsymbol{n} + \bar{\boldsymbol{n}} &= \partial_t \boldsymbol{p} \\ \partial_s \boldsymbol{m} + (\boldsymbol{r} \times \partial_s \boldsymbol{n}) + (\partial_s \boldsymbol{r} \times \boldsymbol{n}) + (\boldsymbol{r} \times \bar{\boldsymbol{n}}) + \bar{\boldsymbol{m}} &= \partial_t \boldsymbol{l}. \end{aligned} \tag{17}$$

Using equation $(17)_1$ together with (13) the following relation can be established

$$\boldsymbol{r} \times \partial_t \boldsymbol{p} = \rho A(\boldsymbol{r} \times \partial_t^2 \boldsymbol{r}) + \boldsymbol{r} \times \partial_t^2 \boldsymbol{q} = \boldsymbol{r} \times \partial_s \boldsymbol{n} + \boldsymbol{r} \times \bar{\boldsymbol{n}}$$

to reformulate equation $(17)_2$ as

$$\partial_s \boldsymbol{m} + \partial_s \boldsymbol{r} \times \boldsymbol{n} + \bar{\boldsymbol{m}} = \partial_t \hat{\boldsymbol{l}} \quad , \tag{18}$$

where $\partial_t \hat{\boldsymbol{l}} = \boldsymbol{q} \times \partial_t^2 \boldsymbol{r} + \partial_t \boldsymbol{h}$ has been introduced. Equation $(17)_1$ and (18) are the 'equations of motion for (the classical form of Cosserat) rods' (cf. [1]). In the following it will be shown, that the classical equations of motion for Cosserat rods fits into the framework introduced in Section 1. For this, the contact forces and moments can be written alternatively as

$$\boldsymbol{n} = N_i \boldsymbol{d}_i = N_i \bar{\boldsymbol{\Lambda}} \boldsymbol{e}_i \quad \text{and} \quad \boldsymbol{m} = M_i \bar{\boldsymbol{\Lambda}} \boldsymbol{e}_i.$$

Focusing on hyperelastic materials, the constitutive relations are governed by the stored energy function $\Psi = \hat{\Psi}(\boldsymbol{\gamma}, \boldsymbol{\kappa})$. We assume that

$$\begin{aligned} N_i &= \partial_{\gamma_i} \Psi(\boldsymbol{\gamma}, \boldsymbol{\kappa}) = \hat{N}_i(\boldsymbol{\gamma}, \boldsymbol{\kappa}) = F_{ik}(\boldsymbol{\gamma}, \boldsymbol{\kappa}) \gamma_k \\ M_i &= \partial_{\kappa_i} \Psi(\boldsymbol{\gamma}, \boldsymbol{\kappa}) = \hat{M}_i(\boldsymbol{\gamma}, \boldsymbol{\kappa}) = G_{ik}(\boldsymbol{\gamma}, \boldsymbol{\kappa}) \kappa_k \end{aligned}$$

holds. Note that the fundamental conditions, regarding the limiting deformation cases, have to be fullfilled. E.g. for $\gamma_\alpha \to \{\pm\infty\}$ the contact force N_α should tend to $\pm\infty$ and the contact force N_3 should tend to $\pm\infty$ for $\gamma_3 \to \{\infty, 0\}$. The contact moments M_i should tend to $\pm\infty$ as the curvature κ_i tends to an upper or lower bound, where an intersection of neighboring cross-sections is imminent. Taking the kinematical relations

$$\gamma_k = \partial_s \boldsymbol{r} \cdot \bar{\boldsymbol{\Lambda}} \boldsymbol{e}_k \quad \text{and} \quad \kappa_k = \partial_s \boldsymbol{\Theta} \cdot \bar{\boldsymbol{\Lambda}} \boldsymbol{e}_k$$

into account, the contact force can be written as

$$\boldsymbol{n} = F_{ik}(\boldsymbol{\gamma}) \gamma_k (\bar{\boldsymbol{\Lambda}} \boldsymbol{e}_i) = (\bar{\boldsymbol{\Lambda}} \boldsymbol{F}^T \bar{\boldsymbol{\Lambda}}^T) \cdot \partial_s \boldsymbol{r}.$$

Herein, $\boldsymbol{F} = F_{ik}(\gamma)(\boldsymbol{e}_i \otimes \boldsymbol{e}_k)$ has been introduced and use of $\boldsymbol{A}\boldsymbol{e}_j \otimes \boldsymbol{A}\boldsymbol{e}_i = \boldsymbol{A}(\boldsymbol{e}_i \otimes \boldsymbol{e}_j)\boldsymbol{A}^T$ has been made [3]. For the contact moment, it follows similarly that $\boldsymbol{m} = (\bar{\boldsymbol{\Lambda}} \boldsymbol{G}^T \bar{\boldsymbol{\Lambda}}^T) \cdot \partial_s \boldsymbol{\Theta}$. With

$$\partial_t^2 \boldsymbol{d}_\alpha = \boldsymbol{S}_{\boldsymbol{\omega}}^2 \boldsymbol{d}_\alpha - \boldsymbol{d}_\alpha \times \partial_t \boldsymbol{\omega}$$

the time derivative of the linear momentum relative to $\boldsymbol{r}(s,t)$ can be written as

$$\partial_t^2 \boldsymbol{q}(s,t) = \boldsymbol{S}_\omega^2 \boldsymbol{q} - \boldsymbol{S}_{\boldsymbol{q}} \partial_t^2 \boldsymbol{\Theta} \quad ,$$

where $\boldsymbol{S}_{(\cdot)}$ denotes the skew symmetric matrtix

$$\boldsymbol{S}_{(\cdot)} = \begin{bmatrix} 0 & -(\cdot)_3 & (\cdot)_2 \\ (\cdot)_3 & 0 & -(\cdot)_1 \\ -(\cdot)_2 & (\cdot)_1 & 0 \end{bmatrix}.$$

Hence, the balance of linear momentum $(17)_1$ can be written as

$$(\rho A) \partial_t^2 \boldsymbol{r} - \boldsymbol{S}_{\boldsymbol{q}} \partial_t^2 \boldsymbol{\Theta} - \partial_s \left(\boldsymbol{\Lambda} \boldsymbol{F}^T \boldsymbol{\Lambda}^T \partial_s \boldsymbol{r} \right) = \bar{\boldsymbol{n}} - \boldsymbol{S}_{\boldsymbol{\omega}}^2 \boldsymbol{q}.$$

[3] This property follows directly from the definition of the dyadic product $(\boldsymbol{a} \cdot \boldsymbol{b})\boldsymbol{c} = (\boldsymbol{c} \otimes \boldsymbol{a})\boldsymbol{b}$

Furthermore, by using the relation for the angular momentum relative to $\boldsymbol{r}(s,t)$ and its time derivative

$$\partial_t \boldsymbol{h}(s,t) = \rho I_{\alpha\beta} \partial_t (\boldsymbol{d}_\alpha \times \partial_t \boldsymbol{d}_\beta) \quad ,$$

equation $(17)_2$ can be written by defining $\boldsymbol{J} \equiv I_{\alpha\beta} \boldsymbol{S}_{\boldsymbol{d}_\alpha} \boldsymbol{S}_{\boldsymbol{d}_\beta}$ and $\boldsymbol{k} \equiv I_{\alpha\beta}(\boldsymbol{d}_\alpha \times \boldsymbol{S}_\omega^2 \boldsymbol{d}_\beta + \boldsymbol{\omega} \cdot (\boldsymbol{d}_\alpha \times \boldsymbol{d}_\beta)\boldsymbol{\omega})$ as

$$\boldsymbol{S}_{\boldsymbol{q}} \partial_t^2 \boldsymbol{r} - \rho \boldsymbol{J} \partial_t^2 \boldsymbol{\Theta} + \boldsymbol{\Lambda} \boldsymbol{G}^T \boldsymbol{\Lambda}^T = \partial_s \boldsymbol{r} \times \boldsymbol{n} + \bar{\boldsymbol{m}} - \rho \boldsymbol{k}.$$

By introducing the coefficients

$$\boldsymbol{A} = \begin{bmatrix} \rho A \boldsymbol{I} & -\boldsymbol{S}_{\boldsymbol{q}} \\ \boldsymbol{S}_{\boldsymbol{q}} & -\rho \boldsymbol{J} \end{bmatrix} \quad \boldsymbol{B} = \begin{bmatrix} \bar{\boldsymbol{\Lambda}} \boldsymbol{F}^T \bar{\boldsymbol{\Lambda}}^T & \boldsymbol{0} \\ \boldsymbol{0} & \bar{\boldsymbol{\Lambda}} \boldsymbol{G}^T \bar{\boldsymbol{\Lambda}}^T \end{bmatrix} \quad \boldsymbol{C} = \begin{bmatrix} \bar{\boldsymbol{n}} - \boldsymbol{S}_{\boldsymbol{\omega}}^2 \boldsymbol{q} \\ (\partial_s \boldsymbol{r} \times \boldsymbol{n}) + \bar{\boldsymbol{m}} - \rho \boldsymbol{k} \end{bmatrix}$$

the problem fits into the framework presented in the beginning of this Section. Note that by definition $\boldsymbol{S}_{\boldsymbol{\omega}} \boldsymbol{\omega} \equiv \boldsymbol{0}$.

Example 1.2 *(Planar problem) Assuming a straight reference configuration* $\boldsymbol{S}_{\boldsymbol{q}} = \boldsymbol{0}$ *and regarding the following strain energy function*

$$\Psi = \frac{1}{2}\left(EI\kappa_2^2 + GA\gamma_1^2 + \frac{EA}{2}(\gamma_3^2 - 2\ln\gamma_3 - 1)\right) \tag{19}$$

the coefficients of the PDE at hand (1) *can be identified as*

$$\boldsymbol{A} = \begin{bmatrix} \rho A & 0 & 0 \\ 0 & \rho A & 0 \\ 0 & 0 & \rho I \end{bmatrix} \quad ; \quad \boldsymbol{C} = \begin{bmatrix} \bar{n}_1 \\ \bar{n}_3 \\ \bar{m}_2 + (\partial_s r_3 n_1 - \partial_s r_1 n_3) \end{bmatrix} \tag{20}$$

and

$$\boldsymbol{B} = \frac{EA}{2}(1-\nu^{-2}) \begin{bmatrix} \cos^2\Theta & \cos\Theta\sin\Theta & 0 \\ \cos\Theta\sin\Theta & \sin^2\Theta & 0 \\ 0 & 0 & 0 \end{bmatrix} + \begin{bmatrix} GA\sin^2\Theta & -GA\cos\Theta\sin 2\Theta & 0 \\ -GA\cos\Theta\sin 2\Theta & GA\cos^2\Theta & 0 \\ 0 & 0 & EI \end{bmatrix}.$$

2 SEQUENTIAL SPACE-TIME INTEGRATION

Classically initial boundary value problems of the form (1) are solved sequentially in space and time, e.g. after the underlying partial differential equation (1) is integrated in space by applying common methods such as the finite element method, the semi-discrete system of equations can be integrated in time by using appropriate time-stepping schemes that are commonly based on finite difference approximations. Following this common procedure we show that the inverse dynamics problem under consideration can be transferred to discrete equations of motion subjected to servo constraints. For this we consider the pure Neumann problem, i.e. neclecting the Dirichlet boundary conditions. An equivalent weak form of the boundary value problem at hand can be accomplished by multiplying $(1)_1$ by sufficiently smooth test functions, integrating subsequently over the spatial domain S, applying integration by parts and taking finally the given Neumann boundary conditions into account. A spatial discretization of the weak form by applying standard finite element approxmations to the vector valued test and trial functions leads to the semi discrete equations of motion. Boundary conditions pertaining the configuration space may be taken into account by imposing geometric constraints. The motion of the constrained mechanical system is then governed by the following semi-explicit differential algebraic system of equations

$$\begin{aligned} \boldsymbol{M}\ddot{\boldsymbol{q}} + \boldsymbol{F}(\dot{\boldsymbol{q}}, \boldsymbol{q}, t) + \boldsymbol{G}^T \boldsymbol{f}(t) = \boldsymbol{0} \\ \boldsymbol{g}(t, \boldsymbol{q}) = \boldsymbol{H}\boldsymbol{q} - \boldsymbol{\gamma}(t) = \boldsymbol{0} \end{aligned} \tag{21}$$

where $\boldsymbol{q} : T \mapsto \mathbb{R}^{d \cdot n_{nodes}}$ denotes the nodal configuration vector that contains the nodal position vectors at time $t \in T$ of the discrete problem at hand. And $\boldsymbol{f} : T \mapsto \mathbb{R}^d$ are the Lagrange multipliers enforcing the given constraints. In case of ordinary contact constraints the Lagrange multipliers are orthogonal to the constraint manifold, e.g $rank(\boldsymbol{H}\boldsymbol{M}^{-1}\boldsymbol{G}^T) = d \cdot n_{nodes}$ holds. Such systems can be identified as DAEs in Hessenberg form of differentiation index 3 by introducing the velocity $\boldsymbol{v} \equiv \dot{\boldsymbol{q}}$ (cf. [18], Chapter 4, p.172). The semi discrete equation of motion can then be solved by integrating (21) subsequently in time by applying suitable finite difference schemes (see, for example, [17]). In contrast to that, the DAEs governing the motion of discrete mechanical systems subject to servo constraints have to be distinguished from those subjected to ordinary contact constraints. Servo constraints often lead to a non-orthogonal constraint realization, where $rank(\boldsymbol{H}\boldsymbol{M}^{-1}\boldsymbol{G}^T) \neq d \cdot n_{nodes}$ holds in general. DAEs with non-orthogonal constraint-realization are often characterised by differentiation index that are higher then 3 (cf. [9], [10], [11]). We've recently shown in [8] that the sequential space-time discretization approach to solve the inverse dynamics problem of flexible systems yields DAEs whose index tends to be excessively high thus hindering a stable numerical solution. In addition to that, the demands on the smoothness of the prescribed trajectory tend to be excessively high as well. In contrast to the simultaneous integration, we could also show in [8], by means of a geometrically exact rope formulation, that due to the hyperbolic nature of the underlying partial differential equation a simultaneous discretization in space and time is much better suited to successfully solve the inverse dynamics problem under consideration. For this purpose, a brief repetition of the simultaneous space-time discretization strategies for the inverse dynamics of spatially continuous systems, introduced firstly in [8], is given in the subsequent Section 3. Herein, we will adress the wave phenomena of hyperbolic equations such as (1) which intuitively motivates the simultaneous space-time integration of the inverse dynamics problem at hand.

3 SIMULTANEOUS SPACE-TIME INTEGRATION

Due to the highly restrictive applicability of solving the control problem at hand sequentially in time, two methods will be presented in this Section, that are based on a simultaneous space-time integration. This will be motivated by the hyperbolic structure of the underlying initial boundary value problem. For this, the classical method of characteristics will be introduced in the subsequent Section.

Method of characteristics. The method of characteristics is based on a geometric interpretation of quasi-linear partial differential equations (cf. [13, 16, 15, 12, 14]). For this the wave equation for the control problem at hand (1) is transformed into a system of first order partial differential equations by introducing the velocity $\boldsymbol{v}(s,t) = \partial_t \boldsymbol{x}(s,t)$ and the deformation gradient

$\boldsymbol{p}(s,t) = \partial_s \boldsymbol{x}(s,t)$

$$\boldsymbol{A}\partial_t \boldsymbol{v} - \partial_s(\boldsymbol{B}\boldsymbol{p}) = \boldsymbol{C} \tag{22}$$

$$\boldsymbol{B}\partial_t \boldsymbol{p} - \boldsymbol{B}\partial_s \boldsymbol{v} = \boldsymbol{0}. \tag{23}$$

With $\boldsymbol{B}\partial_t\boldsymbol{p} = \partial_t(\boldsymbol{B}\boldsymbol{p}) - \partial_t\boldsymbol{B}\boldsymbol{p}$ equation (23) can be written as $\partial_t(\boldsymbol{B}\boldsymbol{p}) - \boldsymbol{B}\partial_s\boldsymbol{v} = \partial_t\boldsymbol{B}\boldsymbol{p}$. Together with

$$\partial_t \boldsymbol{B}(\boldsymbol{p}(s,t)) = (\partial_{\boldsymbol{p}} \otimes \boldsymbol{B}) \cdot \partial_t \boldsymbol{p} = \mathrm{grad}_{\boldsymbol{p}}(\boldsymbol{B}) \cdot \partial_t \boldsymbol{p}$$

and by using the equality of mixed partials $\partial_t\boldsymbol{p} = \partial_s\boldsymbol{v}$ it follows that

$$\partial_t(\boldsymbol{B}\boldsymbol{p}) - \boldsymbol{B}\partial_s\boldsymbol{v} = (\partial_{\boldsymbol{p}} \otimes \boldsymbol{B})\boldsymbol{p}\partial_s\boldsymbol{v} \tag{24}$$

holds. Equation (22) is forming together with (24) and

$$\boldsymbol{B} + (\partial_{\boldsymbol{p}} \otimes \boldsymbol{B})\boldsymbol{p} = \boldsymbol{H}(\boldsymbol{p}) : \bar{\Omega} \mapsto \mathbb{R}^{d,d} \tag{25}$$

a system of first order partial differential equations. Introducing $\boldsymbol{z} : \Omega \mapsto \mathbb{R}^{2d}$, $\boldsymbol{F} : \bar{\Omega} \mapsto \mathbb{R}^{2d}$, $\boldsymbol{D} : \bar{\Omega} \mapsto \mathbb{R}^{2d,2d}$ and $\boldsymbol{E} : \bar{\Omega} \mapsto \mathbb{R}^{2d,2d}$, this system can be written compactly as:

$$\boldsymbol{D}\partial_t\boldsymbol{z} + \boldsymbol{E}\partial_s\boldsymbol{z} = \boldsymbol{F}. \tag{26}$$

Assuming there exists a line $s = k(t)$ along which a solution $\boldsymbol{z} = \boldsymbol{z}(k(t),t) = \boldsymbol{z}_0(t)$ is given. Then this line is called a characteristic line if the partial derivatives of the solution cannot be uniquely determined through informations along this given line. This means that

$$\left(\boldsymbol{E} - \boldsymbol{D}\frac{d}{dt}k(t)\right)\partial_s\boldsymbol{z} = \boldsymbol{F} - \boldsymbol{D}\frac{d}{dt}\boldsymbol{z}_0(t) \tag{27}$$

cannot be solved uniquely for the partial derivatives $\partial_s\boldsymbol{z}$ and $\partial_t\boldsymbol{z}$. Hence, according to Cramers rule

$$\det(\boldsymbol{Q}) = 0 \qquad \text{and} \qquad \det_i(\boldsymbol{Q}) = 0 \tag{28}$$

has to hold for the coefficient matrix $\boldsymbol{Q} = \boldsymbol{E} - \boldsymbol{D}\frac{d}{dt}k(t)$ as well as for the matrix $\boldsymbol{Q}_i$, where the i-th column is replaced by the right hand side $\boldsymbol{F} - \boldsymbol{D}\frac{d}{dt}\boldsymbol{z}_0(t)$. The wave equation could thus be transformed into a system of ordinary differential equations along characteristic lines. This system can be solved numerically by using e.g. appropriate finite difference schemes.

Example 3.1 *(Planar problem - contd.) The wave propagation within the planar formulation of the geometrically exact beam (cf. Example 1.2) can be analysed by evaluating*

$$(\partial_{\boldsymbol{p}} \otimes \boldsymbol{B})\boldsymbol{p} = \frac{EA}{\nu^2}\begin{bmatrix} \cos^2\Theta & \cos\Theta\sin\Theta & 0 \\ \cos\Theta\sin\Theta & \cos^2\Theta & 0 \\ 0 & 0 & 0 \end{bmatrix} \tag{29}$$

and

$$\boldsymbol{H} = \frac{EA}{2}(1+\nu^{-2})\begin{bmatrix} \cos^2\Theta & \cos\Theta\sin\Theta & 0 \\ \cos\Theta\sin\Theta & \sin^2\Theta & 0 \\ 0 & 0 & 0 \end{bmatrix} + \begin{bmatrix} GA\sin^2\Theta & -GA\cos\Theta\sin 2\Theta & 0 \\ -GA\cos\Theta\sin 2\Theta & GA\cos^2\Theta & 0 \\ 0 & 0 & EI \end{bmatrix}$$

for the given coefficients. The directionality condition (28) *leads then to*

$$c_1 = \pm\left(\frac{EI}{\rho I}\right)^{\frac{1}{2}}, \quad c_2 = \pm\left(\frac{GA}{\rho A}\right)^{\frac{1}{2}} \quad \textit{and} \quad c_3 = \pm\left(\frac{1}{2}\frac{EA}{\rho A}\left(1+\frac{1}{\nu^2}\right)\right)^{\frac{1}{2}}. \tag{30}$$

Here, c_i can be identified as the speed of wave propagation corresponding to bending ($i = 1$), shear ($i = 2$) and elongation ($i = 3$), respectively. It is worth to mention, that the compatibility condition $(28)_2$ *yields a system of ordinary differential equations along the characteristic lines* $(28)_1$*. Following [8] and references therein, this system of ODEs can be solved globally in the space-time domain* Ω*.*

Space-time finite element method. Due to the gained insights of the underlying wave dominated problems, a space-time finite element method will be presented in this paragraph. For further information we would like to refer to [8] as well as [5], [6] and [7]. By introducing the velocity $\boldsymbol{v}(s,t) = \partial_t \boldsymbol{x}(s,t)$, the underlying partial differential equation at hand (1) can be transformed into a system of partial differential equations, that is first order in time:

$$\begin{aligned} \partial_t \boldsymbol{x} - \boldsymbol{v} &= \boldsymbol{0} \\ \boldsymbol{A}\partial_t \boldsymbol{v} - \partial_s(\boldsymbol{B}\partial_s \boldsymbol{x}) &= \boldsymbol{C}. \end{aligned} \tag{31}$$

Multiplying each equation in (31) with sufficiently smooth test functions $\boldsymbol{w}_1(s,t)$ and $\boldsymbol{w}_2(s,t)$, integrating over the space-time domain $\Omega = S \times T$ and applying integration by parts to the second integral of $(31)_2$ regarding the spatial variable

$$\int_\Omega \boldsymbol{w}_2 \cdot \partial_s(\boldsymbol{B}\partial_s \boldsymbol{x})\, d\Omega = \int_T \left[\boldsymbol{w}_2 \cdot \boldsymbol{B}\partial_s \boldsymbol{x}\right]_{s=0}^1 dt - \int_\Omega \partial_s \boldsymbol{w}_2 \cdot \boldsymbol{B}\partial_s \boldsymbol{x}\, d\Omega \tag{32}$$

yields the following weak formulation:

$$\begin{aligned} \int_\Omega \boldsymbol{w}_1 \cdot \left(\partial_t \boldsymbol{x} - \boldsymbol{v}\right)\, d\Omega &= \boldsymbol{0} \\ \int_\Omega \boldsymbol{w}_2 \cdot \boldsymbol{A}\partial_t \boldsymbol{v}\, d\Omega - \int_T \left[\boldsymbol{w}_2 \cdot \boldsymbol{B}\partial_s \boldsymbol{x}\right]_{s=0}^1 \mathrm{d}t + \int_\Omega \partial_s \boldsymbol{w}_2 \cdot \boldsymbol{B}\partial_s \boldsymbol{x}\, d\Omega &= \int_\Omega \boldsymbol{w}_2 \cdot \boldsymbol{C}\, d\Omega. \end{aligned} \tag{33}$$

Additionally the servo-constraint $\boldsymbol{g}_c(t) = \boldsymbol{x}(s=1,t) - \boldsymbol{\gamma}(t)$ can be demanded weakly on the boundary $\partial\Omega_{\boldsymbol{\gamma}} = \{1\} \times T$

$$\int_{\partial\Omega_\gamma} \boldsymbol{w}_3(t) \cdot \boldsymbol{g}_c(t)\, dt = 0. \tag{34}$$

The task is now to find the unknown functions

$$\begin{aligned} \boldsymbol{x}(s,t) &\in V_1 = \left\{\boldsymbol{x} : \Omega \mapsto \mathbb{R}^d \,|\, \boldsymbol{x}(\partial\Omega_0) = \boldsymbol{x}_0\right\} \\ \boldsymbol{v}(s,t) &\in V_2 = \left\{\boldsymbol{v} : \Omega \mapsto \mathbb{R}^d \,|\, \boldsymbol{v}(\partial\Omega_0) = \boldsymbol{v}_0\right\} \\ \boldsymbol{f}(t) &\in V_3 = \left\{\boldsymbol{f} : \partial\Omega_f \mapsto \mathbb{R}^d \,|\, \boldsymbol{f}(\partial\Omega_f \cap \partial\Omega_0) = \boldsymbol{f}_0\right\} \end{aligned}$$

such that for arbitrary but sufficiently smooth test functions

$$\boldsymbol{w}_1(s,t), \boldsymbol{w}_2(s,t) \in W_1 = \Big\{\boldsymbol{w}_1, \boldsymbol{w}_2 : \Omega \mapsto \mathbb{R}^d \,|\, \boldsymbol{w}_1(\partial\Omega_0) = 0, \boldsymbol{w}_2(\partial\Omega_0) = 0\Big\}$$
$$\boldsymbol{w}_3(t) \in W_2 = \Big\{\boldsymbol{w}_3 : \partial\Omega_\gamma \mapsto \mathbb{R}^d \,|\, \boldsymbol{w}_3(\partial\Omega_\gamma \cap \partial\Omega_0) = 0\Big\}$$

the equations (33) and (34) are satisfied together with the given boundary and initial conditions. The weak formulation consisting of (33) and (34) subjected to the given Neumann and Dirichlet boundary conditions can then be solved numerically using the finite element method based on a piecewise continuous approximation.

Example 3.2 *(Numerical example) Regarding a beam with mass density $\rho = 1$ and axial-, bending- and shear stiffness $EA = 1$, $EI = 1$ and $GA = 1$ respectively, the actuation $\boldsymbol{f} = \begin{bmatrix} f_x & f_y & m \end{bmatrix}^T$ acting at $s = 0$ is searched, such that the beam at $s = L$ follows a prescribed trajectory. Furthermore, the length of the beam is assumed to be $L = 1$ in a stress-free reference configuration. A rest-to-rest maneuver starting at $t_0 = 2$ and ending at $t_f = t_0 + T = 4$ is choosen. The prescribed maneuver can therefore be defined by*

$$\boldsymbol{\gamma} = \begin{bmatrix} 1 \\ 0 \\ 0 \end{bmatrix} \forall t < t_0 \qquad \boldsymbol{\gamma} = \begin{bmatrix} 1 - \cos(\varphi \cdot s(t)) \\ \sin(\varphi \cdot s(t)) \\ \varphi \cdot s(t) \end{bmatrix} \forall t \in [t_0, t_0 + T] \qquad \boldsymbol{\gamma} = \begin{bmatrix} 0 \\ 1 \\ \varphi \end{bmatrix} \forall t > t_f. \tag{35}$$

Here, φ denotes the angle of rotation. Furthermore, the function

$$s(t) = 1 - \frac{1}{2}\left(\cos\left(\frac{\pi}{2}\left(\sin\left(\pi\frac{t - t_0}{T} - \frac{\pi}{2}\right) + 1\right)\right) + 1\right)$$

has been introduced.

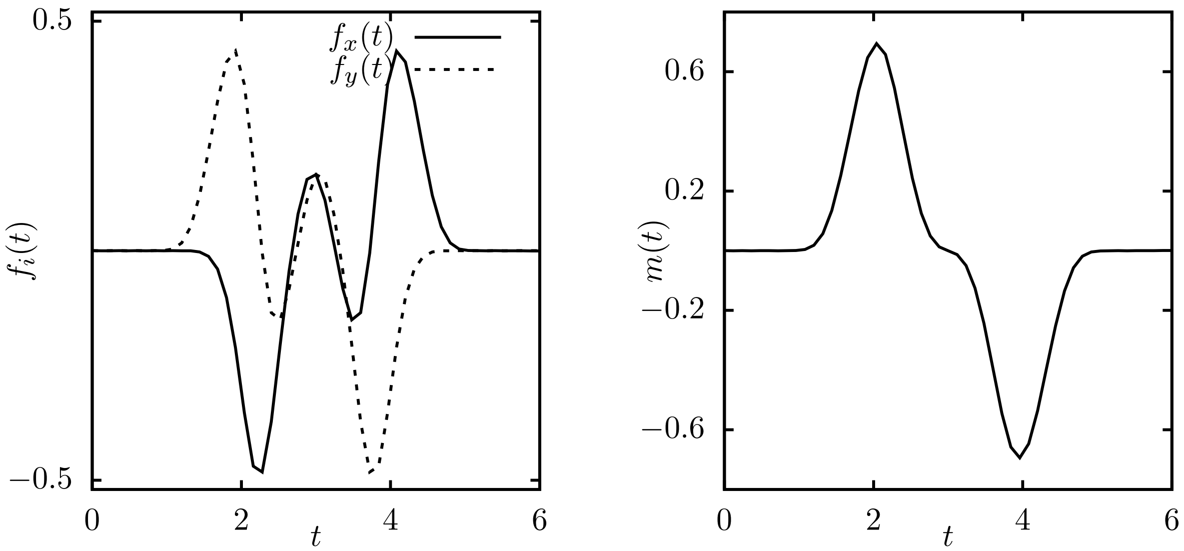

Figure 1: Components of the force (left) and torque (right) acting at $s = 0$ computed with the proposed space-time finite element method such that the beam at $s = L$ follows a prescribed circle from $P_0(1, 0)$ to $P_T(0, 1)$

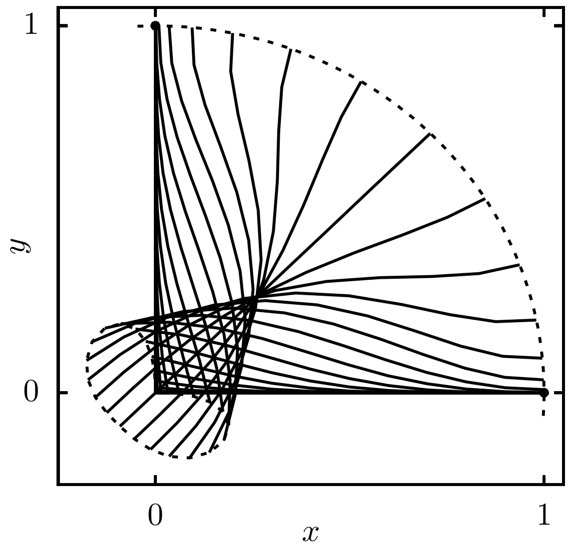

Figure 2: Snapshots of the circular rest-to-rest motion.

In Figure 1 the components of the actuating force f_i (left) and the actuating torque m (right) is depicted. Note, that also the delay time can be observed herein. This is due to the hyperbolic structure of the underlying system mentioned earlier. In Figure 2 snapshots of the planar motion of the beam satisfying the prescribed trajectory at $s = L$ are shown.

4 CONCLUSION

This work deals with the inverse dynamics of flexible mechanical systems whose motion is governed by quasi-linear partial differential equations of hyperbolic type. In Section 1 the initial boundary value problem governing the inverse dynamics of flexible mechanical systems could be introduced abstractly. Then, a brief overview of the basic derivation of the classical equations of motion for the classical form of Cosserat rods, was given and it could be shown that these equations fit into the proposed framework. In the subsequent Section 2, problems that occure by solving the initial boundary value problem at hand by using classical sequential space-time integration methods could be adressed. In particular, the role of the given servo-constraints in causing these problems could be addressed by identifying crucial differences to ordinary contact-constraints. In Section 3 simultaneous space-time integration methods could be presented that are highly motivated by the wave phenomena within elastic media. For this we identified characteristic lines in space-time along that information propagates. Inspired by these insights we presented two methods, namely the method of characteristics and a space-time finite element method, that are capable to solve the inverse dynamics of geometrically exact ropes (cf. [8]) and beams. The abstract formulation of the underlying problem introduced in Section 1 enables an extension of the presented simultaneous space-time integration methods to other flexible mechanical systems such as geometrically exact shells or continua.

REFERENCES

[1] S.S. Antman. *Nonlinear Problems of Elasticity* Vol. 2., (2005). Springer.

[2] J.C. Simo. A finite strain beam formulation. The three-dimensional dynamic problem. Part I. *Computer Methods in Applied Mechanics and Engineering* (1985) **49**:55–70.

[3] E. Reissner. On one-dimensional finite-strain beam theory: The plane problem. *Journal of Applied Mathematics and Physics (ZAMP)* (1972) **23**:795–804.

[4] P. Betsch and P. Steinmann. Frame-indifferent beam finite elements based upon the geometrically exact beam theory. *Int J Numer Methods Eng.* (2002) **54**(12):1775–1788.

[5] J. H. Argyris and D. W. Scharpf. Finite Elements in Time and Space. *Nuclear Engineering and Design* (1969) **10**:456–464.

[6] T. J. R. Hughes and G. M. Hulbert. Space-Time Finite Element Methods for Elastodynamics: Formulations and Error Estimates. *Computer Methods in Applied Mechanics and Engineering* (1988) **66**:339–363.

[7] C. Hesch, S. Schuß, M. Dittmann, S. R. Eugster, M. Favino and R. Krause Variational Space-Time Elements for Large Systems. *Computer Methods in Applied Mechanics and Engineering* (2017) **326**:541–572.

[8] T. Ströhle and P. Betsch. A simultaneous space-time discretization approach to the inverse dynamics of geometrically exact strings. *Int J Numer Methods Eng.* (2022) **123**(11):2573–2609.

[9] W. Blajer and K. Koodziejczyk. A Geometric Approach to Solving Problems of Control Constraints: Theory and a DAE Framework. *Multibody Syst Dyn.* (2004) **11**:343–364.

[10] W. Blajer. Dynamics and control of mechanical systems in partly specified motion. *J. Franklin Inst.* (1997) **334B**:407–426.

[11] R. Seifried and W. Blajer. Analysis of servo-constraint problems for underactuated multibody systems. *Mechanical Sciences* (2013) **4**(1):113–129.

[12] F. John. *Partial Differential Equations* (1982). Springer.

[13] M. B. Abbott. *An Introduction to the Method of Characteristics* (1966). Elsevier.

[14] R. Courant and D. Hilbert. *Methoden der mathematischen Physik II* (1937). Springer.

[15] R. Sauer. *Anfangswertprobleme bei partiellen Differentialgleichungen* (1958). Springer.

[16] R. Courant. *Supersonic Flow and Shock Waves* (1948). Interscience.

[17] B. Leimkuhler and S. Reich. *Simulating Hamiltonian Dynamics* (2004). Cambridge University Press.

[18] P. Kunkel and V. Mehrmann. *Differential-Algebraic Equations - Analysis and Numerical Solution* (2006). EMS Textbooks in Mathematics. European Mathematical Society.